Nigerian Research Journal of Chemical Sciences **(ISSN: 2682-6054)**
Volume 11, Issue 2, 2023

Kinetic and Isotherm Studies of an Anionic Dye (Congo Red) on Cellulose Isolated from Kolanut Pod (*Cola nitida*) Husk

*[1]Adeyemi Lawrence OGUNNEYE, [2]Aderanti Olayemi BADEJO, [1]Muhideen Remilekun GBADAMOSI, [1]Oluwakemi Oluwabunmi BANJOKO, [1]Kehinde Oluwasayo MOYIB, [1]Olumide Frances OLADAPO, [1]Oluwaseun Hannah ANSELM, [1]Babatunde Seun SOTUBO

[1]Department of Chemical Sciences, College of Science and Information Technology, Tai Solarin University of Education, Ijagun, Ogun State, Nigeria

[2]Department of Chemical Sciences, Lagos State University of Education, Ojo, Ijanikin, Lagos State, Nigeria

*Corresponding Author**:** ogunneyeal@tasued.edu.ng

ABSTRACT

As a low-cost adsorbent for the removal of Congo red (CR) dye from aqueous solutions, kolanut pod (*Cola nitida*) husk cellulose, a polymer derived from waste discarded from the kolanut plantation, has been investigated. Functional groups were identified through FTIR spectroscopic investigation on kolanut pod husk cellulose and their binding influence played crucial roles in dye adsorption. The kinetics and isotherms of adsorption were determined using batch experiments. According to experimental findings, at 25 °C, the adsorbent dosage, dye concentration, and pH all increased with the rate of adsorption until optimum points. Adsorption equilibrium was attained in 60 minutes, with an equilibrium efficiency of up to 96.5%. The pseudo-second-order, Elovich (adsorption kinetics), and Langmuir adsorption isotherm models all offered an excellent fit to the experimental data. Results showed that kolanut pod husk cellulose removed dye from industrial effluents in an efficient, environmentally friendly, renewable, and cost-effective manner.

Keywords: Cellulose, anionic dye, Congo red, kinetic, isotherm

INTRODUCTION

A dye is an organic compound that absorbs light in the visible region of electromagnetic radiation. The primary characteristics of dye are its solubility, unstable delocalized electron of aromatic ring, and chromophore-chromogene conjugate system (electron acceptor) [1, 2]. A chromogen is a substance capable of conversion into a pigment or dye by chemical reaction while chromophore is the group in the dye molecular structure that absorb in the visible region of electromagnetic radiation spectrum, causing it to have colours [3-5]. Auxochrome, which

are functional groups, increase the dye's solubility in water [1]. They enhance colour and increase dye's ability to attach to fabrics [6].

In heavy industries, such as those that process paper, textiles, and food, dye is frequently used to colour items [7, 8]. According to reports, the release of hues or various shades in effluent causes 20% of water contamination [9]. Therefore, water contamination brought on by dye release is dangerous and detrimental to the aquatic ecology, food chain, and overall public health [1].

Textile industry effluents exhibit extreme variations in a number of parameters, including BOD, turbidity, colour, COD, pH, odour, and salinity [8, 10, 11]. Azo dyes, such as Congo red, Direct Blue 15, and Direct Red 2, are notorious for being noxious, mutagenic, and carcinogenic [12]. Congo red dye (Figure 1a) possesses significant affinity to fibers made from cellulose and therefore, used in the textile manufacturing industry. Aquatic flora and wildlife become suffocated as a result of dye-contaminated effluent because it lowers oxygen levels in the water and badly affects aquatic plants' ability to photosynthesise [1, 13]. For example, *Chlorella vulgaris*' growth rate and photosynthetic efficiency were significantly affected when exposed to Congo red dye [14]. The need for treating textile effluents polluted with dyes (organic) has become hypercritical because of depleting freshwater resources, expensive treatment costs, and stringent government disposal laws.

Treatment of dye effluent from textile industries is a required but challenging process because they are resistant to conventional treatment due to the complex aromatic composition. Adsorption [15], biological [16], membrane filtration [17], ion exchange [18], biodegradation [19], and electrochemical oxidation [20] are some of the methods currently being used to treat textile effluent contaminated with dyes. Adsorption is currently regarded as one of the most promising techniques due to its effectiveness, simplicity, ease of use, environmental friendliness, and moderate reaction conditions. Adsorption is frequently used to cleanse, pre-concentrate, detoxify, deodorize, and separate liquid and gaseous mixtures in order in order to remove and recover damaging materials [21].

Commercially available activated carbon is widely used as an adsorbent due to its effectiveness and capacity to absorb pollutants [22]. However, it is less desirable as an adsorbent due to its high initial cost, quick saturation, and challenging regeneration. These factors have prompted numerous studies to find less expensive, more environmentally friendly, and more effective adsorbent alternatives. Several cost effective adsorbent like bio-wastes e.g. saw dusts [23], microorganisms like Egyptian water hyacinth [24], biomaterials like Chitosan

[3, 25], modified biomaterials like activated macadamia nutshell [26], bio-wastes like macadamia seed husks [27] and bentonites like natural clays [28, 29] have been researched.

In the region of West Africa, Nigeria produces the most kola nuts [30]. Harvesting involves separating the fruit from its pod, with the pod being thrown away as waste. Over 50% of the kola fruit is made up of the pod husk, which has historically been an agricultural waste. Due to the waste's high moisture content, it easily decomposes when dumped in fields or landfills, having negative environmental effects by creating ideal conditions for the growth of diseases, snails, mosquitoes, and snakes. Hence, there is need to convert waste to wealth.

As a soft wood, kolanut pod husk is thought to be rich in cellulose (Figure 1b), a long-chain polymer made up of repeated D-glucopyranose units and three hydroxyl groups per hydroglucose unit [31]. The presence of these functional groups provides numerous active adsorption sites for adsorption with dyes, heavy metals and other contaminants in solution either in modified or unmodified form.

Therefore, this present study was aimed at synthesizing cellulose from readily available kolanut pod husk. The prepared cellulose adsorbent was applied for the removal of CR dye from aqueous media. The kolanut pod husk cellulose (KPHC) adsorbent was characterized by FTIR for functional group analysis before and after adsorption of CR dye. The effect of various parameters on the dye adsorption onto KPHC adsorbent such as solution pH, adsorbent dosage, contact time, and initial dye concentrations were studied. The isotherm and kinetic data were also evaluated by applying various models.

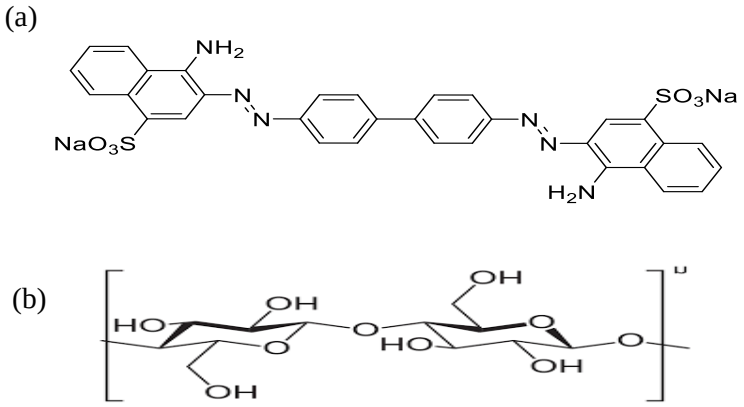

Figure 1: Molecular structure of (a) Congo red (C.I. 22120) and (b) cellulose

Materials and methods

Kolanut pod husks (KPH) (*Cola nitida*) waste were collected from a cocoa plantation in Awa-Ijebu, Ijebu North Local Government Area, Ogun State, Nigeria. The KPH wastes were washed

with water several times to remove adherent dirt, and thereafter dried for 2 -3 weeks to remove moisture. A ball mill machine was used to grind the dried KPH wastes. The cellulose (adsorbent) was prepared from powdered KPH according to the method of Ogunneye *et al*. [31]. The CR dye, a red powdery substance with mass 696.68 g $mol^{-1}$of molecular mass and a maximum absorbance of 497 nm, was obtained from Sigma-Aldrich and utilized without additional purification process.

FT-IR analysis

Functional groups characterisation of KPH cellulose before and after adsorption with CR dye was done by Fourier Transform Infrared Spectrophotometer (Perkin Elmer Spectrum RXI model). The powdered sample was mixed with KBr at an approximate ratio to prepare pellets and afterward put in the sample holder for analysis.

Batch adsorption analysis

Batch sorption assays were performed in a 100 mL conical flask containing 1 g of KPH cellulose and 50 mL of 100 mg L^{-1} CR solution. The resulting mixture was then put on a mechanical shaker and agitated at 150 rpm for an hour. The residual concentration of the dye for each study was measured with an ultraviolet-visible spectrophotometer that operates at a maximum wavelength of 497 nm. Using 1.0 g KPH cellulose, a pH dependent investigation covering the range of pH 2 to 12 was conducted. Dropwise additions of either 0.01M HCl or 0.01M NaOH were used to adjust the pH of the solution. A 100 mL conical flask filled with 50 mL of 100 mg L^{-1} of CR at the optimum pH level was used to study adsorbent dosages of 0.5 to 3.0 g. The effect of contact time was examined by varying the time of agitation from 10 – 180 min of the mixture of CR dye and KPH cellulose adsorbent at optimum pH and dosage while the effect of initial dye concentration was investigated by varying the concentration of CR dye solution from 10 – 100 mg L^{-1} at the optimal pH, dose, and time [32]. At various time intervals, aliquots from the dye mixture were taken, and the residual dye concentration was determined. Using Eqs. (1) and (2), the amount and percent of CR dye removed (q_e) were calculated.

$$q_e = (C_o - C_e)\frac{V}{m} \quad (1)$$

$$\text{Percentage (\%) of CR adsorbed} = \frac{C_o - C_e}{C_e} \times 100 \quad (2)$$

Where "Co" and "Ce" are the liquid-phase concentrations (mg L^{-1}) of dye at initial and equilibrium stages respectively; "V" represents the volume of the solution, (L) and "m" is the mass of KPH cellulose (g).

RESULTS AND DISCUSSION

Isolation of KPH cellulose from KPH waste

The KPH cellulose was successfully isolated from the KPH waste. The KPH cellulose obtained was white and powdery in nature [31].

Characterization of functional group by FTIR

The functional group that was present on the surface of KPH cellulose before and after it was bound to CR dye was revealed by FTIR analysis. Figure 2 displays the KPH cellulose FTIR spectrum and the bands allocated, which are listed in Table 1 as a summary. According to the findings, KPH cellulose has a broad band at 3348.28 cm^{-1} caused by an OH stretching vibration, a C-.H stretch of 2957.85 cm^{-1}, and C=O absorption bands close to 1769.18 cm^{-1}, while the band at 795.67 cm^{-1} is linked to the structure of the cellulose made up of α-linkages of cellulose. Wekoye *et al*. [32] published similar findings in the literature as well. When KPH cellulose adsorbed CR dye, there was a band shift in the functional groups. New spectra peaks on the cellulose appeared at 1502.72 cm^{-1}, which are owing to the -N=N- peak as well as the SO_3-H stretch-induced absorption at 1065.12 cm^{-1} [33].

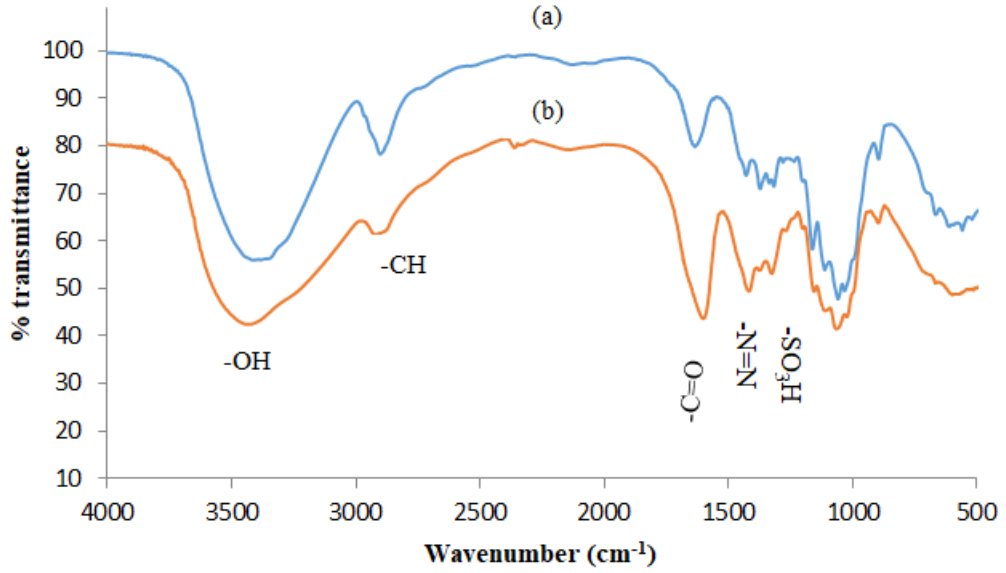

Figure 2**:** FTIR spectra of (a) unloaded KPH cellulose (adsorbent) and (b) loaded KPH cellulose with CR dye

Table 1: FT-IR spectra properties of KPH cellulose loaded and unloaded with CR dye

S/N	KPH Cellulose (Unloaded)	Vibrational mode	KPH loaded with CR	Vibrational mode
1	3348.28	-OH broad band	3473.49	-OH broad band shift
2	2957.85	-CH stretching	2989.46	-CH stretching
3	1769.18	-C= O bending vibration	1502.72	-N=N- stretching vibration
4	1429.49	$-CH_2$ scissoring	1043.43	SO_3-H stretching
5	1148.72	C-O-C stretching		
6	795.67	-1,4-glycosidic bond	1065.12	S=O of sulfonic acid Stretching vibration

Effect of pH

In the adsorption process, pH is crucial because it controls the charges on the adsorbent material and the dye molecules ionization [34]. According to Chowdhury *et al.* [34], it was directly related to H^+ ability to compete for the active sites on adsorbent surfaces with dye molecules. KPH cellulose was used to test the effect of pH on the adsorption of CR dye, and the findings are shown in Figure 3a. As a result of the positive charge on the CR molecule, which was attached to one another by a repulsive attraction, the percentage (%) adsorption of CR at equilibrium increased with as pH rise until it reach to pH 8 and then started to decline. Similar results were seen when Basic Yellow 28 (BY28) was removed from natural clays that were rich in smectite [35].

Effect of KPH cellulose dose

The amount of dye removed and the rate of adsorption are significantly influenced by the dosage of the adsorbent [36]. The findings of evaluating the effect of KPH cellulose dose on the sorption of CR dye are shown in Figure 3b. Increase in KPH cellulose adsorbent dose led to improvement in the % dye adsorbed. For instance, when KPH cellulose dosages were raised from 0.50 to 2.50 g, the percentage of CR adsorbed increased from 91.5 to 96.5% respectively. Therefore, the optimum dose is 2.5 g. This result was explained by the fact that as the KPH cellulose dose increased, there was a significant rise in the number of adsorption locations that the dye could access, leading to a larger % of adsorption [37]. A similar pattern was observed in the use of activated carbon for the adsorption of the dye bromophenol blue, where an increase in activated carbon dose led to an increase in dye removal [38].

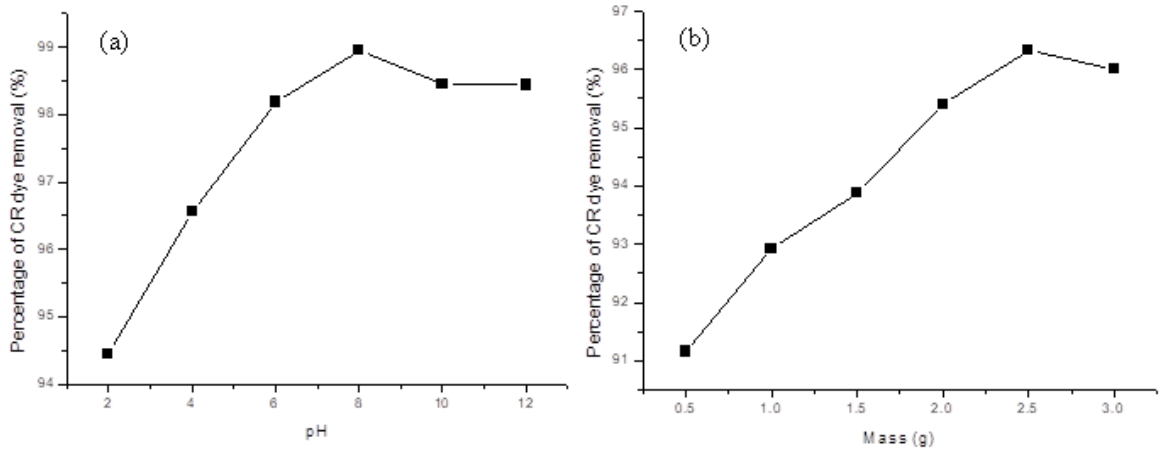

Figure 3: (a) pH effect on percentage removal of CR dye by KPH cellulose adsorbent (100 mg L^{-1} of CR dye; KPH dose 1.0 g; time 60 min) (b) Effect of KPH cellulose adsorbent dosage on CR dye removal (CR dye 100 mg L^{-1}; pH 8; time 60 min at 25 °C).

Effect of contact time

In industrial settings, contact time is crucial since it influences the method's cost-effectiveness and maximal treatment time. Figure 4(a) shows the findings from the investigation on the impact of contact time on CR dye removal. It is clear that the experiment's dye removal rate started off quickly before progressively slowing till equilibrium. Therefore, the optimum contact time for the experiment is 60 min. The observation can be explained by the fact that there were fewer vacant sites on the adsorbent over time until they were completely taken up at equilibrium. Both the adsorption of CR dye utilizing root of *Eichhornia crassipes* and the

removal of Acid red 1 dye using chemically altered sugarcane bagasse have yielded similar results [32, 36].

Effect of initial dye concentration

Figure 4b displays the results of investigating the impacts of CR dye concentration at various concentrations. A greater amount of CR was adsorbed at equilibrium when the initial concentration of the CR dye was higher. For instance, the quantity of CR removed at equilibrium rose from 0.25 to 2.0 mg g^{-1} when the CR concentration increased from 10 to 60 mg L^{-1}. The observed phenomenon can be explained by the higher concentration slope between the liquid and adsorbent phases that are present at higher concentrations, boosting the adsorption rate [39]. However, as dye concentration increased, the adsorption effectiveness decreased as KPH cellulose's adsorption sites quickly became saturated. Similar results have been reported for the adsorption of malachite green and Congo red using corn stalk bio-waste material and the crystal violet dye removal utilizing husks of coffee [40].

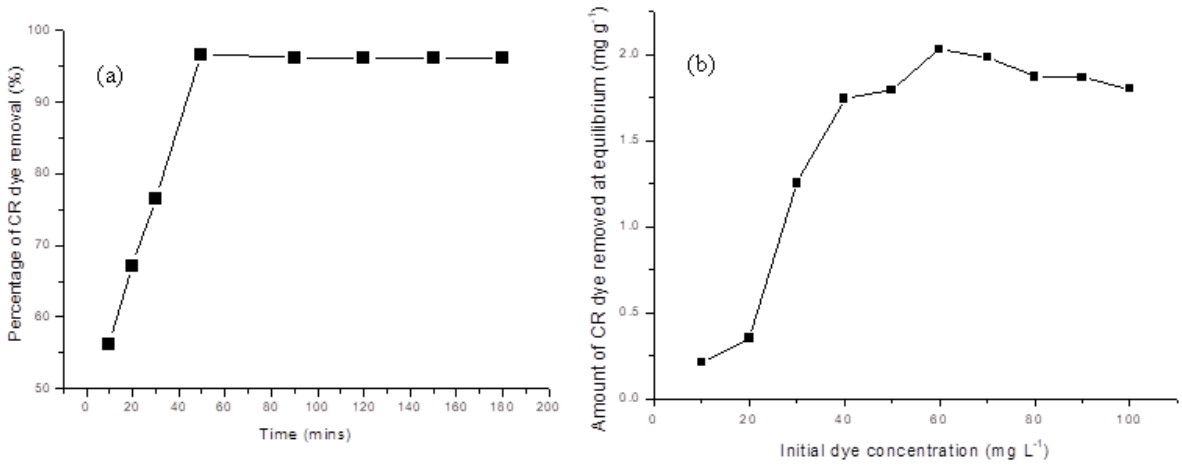

Figure 4: (a) Contact time effect on the CR dye adsorption of (100 mg L^{-1} CR, 2.5 g KPH cellulose dose, and pH of 8) (b) Effect of the initial concentration of CR on the quantity of dye removed (pH 8, time 60, 2.5 g dose min at 25 °C).

Isotherms adsorption

Adsorption isotherms are important when developing a treatment system for wastewater. Langmuir and Freundlich isotherms were used to assess viability of CR dye removal from solutions. Monolayer adsorption processes are described using the Langmuir adsorption isotherm [41]. The assumption is that adsorptions take place on homogeneous, uniform surface

with identical areas on the adsorbent. The equation for the linearized variants of the Langmuir isotherm is as follows:

$$\text{Langmuir: } \frac{1}{q_e} = \frac{1}{q_{max}} K_{LY}\left(\frac{1}{C_e}\right) + \frac{1}{q_{max}} \quad (3)$$

where q_e is the amount Congo red dye removed at equilibrium (mg g^{-1}), C_e is the Congo red concentration at equilibrium, Q_{max} is the adsorption capacity mono layer (mg g^{-1}), and K_{LY} denote constant for Langmuir (mg L). The point intercepts and gradients from the 1/qe vs. 1/Ce plots are used to determine Qmax and Langmuir constant (KLY).

Figure 5a depicts the plot of 1/qe against 1/Ce for CR removal onto KPH cellulose. According to the results, a mono layer adsorption capacity (Qmax) of 4.21 mg g^{-1} was attained with a KLY of 2.655 mg L and R^2 of 0.894.

The Freundlich isotherm [17] is applicable to multilayer sorption and non-ideal sorption on heterogeneous surfaces. The equation's linearized form is written as: Freundlich:

$$\log q_e = \frac{1}{n}\log C_e + \log K_f \quad (4)$$

where k_f is the adsorbent capacity and n refer to the intensity of the adsorption, respectively. The intercepts (logkf) and slopes (1/n) of the plot of log qe against Iog Ce provide the values for kf and n. The adsorption process is rated favourably by 1/n, and if an n value is greater than 1, it implies suitable adsorption conditions. Figure 5b depicts the log q_e vs Iog C_e plot for the CR dye removal by KPH cellulose. According to the findings, an adsorption intensity (n) value of 1.632 and an R^2 of 0.988 were used to produce the Freundlich constant similar to adsorption capacity (k_f) of 1.654 (mg g^{-1}) (L mg^{-1})n^{-1}). Furthermore, since the value of n (1.632) is greater than 1, therefore the adsorption process is favourable. In conclusion, the suitability of a particular model is determined by the coefficient of determination, R^2, which measures the conformation of the regression line to the experimental data. A perfect fit is indicated by unity, although a value close to unity can be an indication of good fit. Values < 0.8 expresses the inadequacy of such a model in explaining the experimental data [42]. High R^2 ($R^2 \geq 0.8$) values for both the Langmuir and Freundlich adsorption isotherm models allow us to infer that both monolayer and multilayer adsorption processes occurred at 25 °C [43]. Although the Langmuir isotherm (Figure 5a) model also demonstrated good fit of the experimental data, but Freundlich

adsorption isotherm model (Figure 5b) demonstrated better fit than Langmuir isotherm due to its R^2 value.

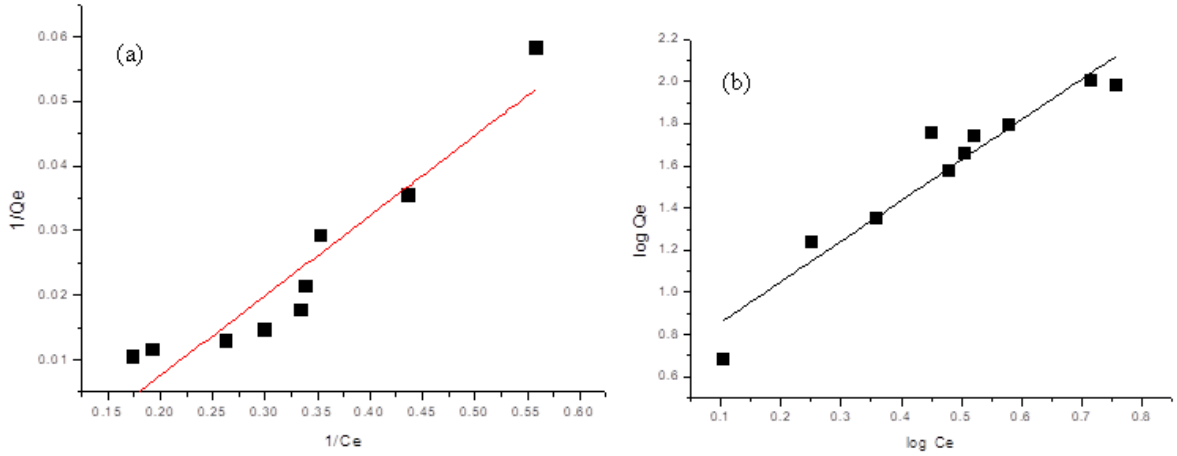

Figure 5: (a) Langmuir isotherm plot for CR on KPH cellulose (b) Freundlich isotherm plot for CR on KPH cellulose

Adsorption kinetics

The chemical pathways and possible rate-limiting stages for the removal of CR on KPH cellulose were investigated using pseudo-first and pseudo-second order kinetic models and the Elovich equation. The linearized integral version of the Lagergren pseudo-first-order model [1] is provided in Equation 5:

Lagergren pseudo-first order: $log(q_e - q_t) = logq_e - \left(\frac{K_1}{2.303}\right)t$ (5)

Where, correspondingly, q_e and q_t are the amounts of dye removed at equilibrium (mg g^{-1}) with respect to time (min), k_1 is the pseudo-first-order adsorption constant (min^{-1}). The gradient and intercepts of log (q_e - q_t) versus t are used to derive the k_1 and q_e values (figure 6a). Low R^2 values ($R^2 < 0.5$) indicated a poor fit of the experimental data by the pseudo-first order kinetic model. The inadequacy of the model in representing the CR's adsorption on KPH cellulose was shown in Table 2.

The adsorption of CR dye onto KPH cellulose was also investigated using a pseudo-second order model. The pseudo-second order model's linear equation is stated in Equation 6:

Pseudo-second order: $\frac{t}{qt} = \frac{1}{k_2 q_e^2} + \left(\frac{1}{q_e}\right)t$ (6)

Where q_e and q_t refer to the dye adsorbed at equilibrium and time t (mg g^{-1}), respectively, and k_2 is the adsorption rate constant (g mg min^{-1}). The intercepts and gradient of t/qe vs. t are used to derive the values of k_2 and q_e. Figure 6b displays the plot of pseudo-second order kinetics for the adsorption of CR dye onto KPH cellulose at various time (mins). The model had a good fit with the experimental data. Table 2 lists the values of k_2, q_e, and R^2 after they have been calculated. High R^2 values ($R^2 > 0.8$) were found for the concentrations under study. The outcome demonstrates that CR dye was adsorbed by KPH cellulose according to a pseudo-second order kinetic model. This further shows that chemisorption, which involves the exchange or sharing of electrons between the adsorbent and adsorbate, increased the adsorption process [44-45].

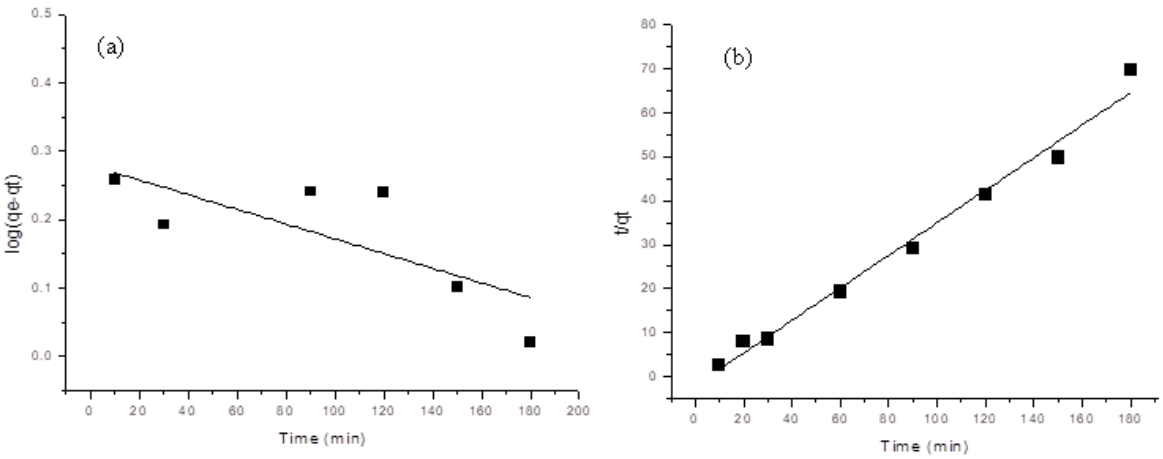

Figure 6 (a) Pseudo-first order model and (b) Pseudo-second order model plots for adsorption of CR dye on KPH cellulose.

Elovich's equation was used to further examine the CR dye's adsorption on KPH cellulose [46]:

Elovich: $q_t = A + B\ln t$ (7)

Where qt is the quantity (mg g^{-1}) of CR that has been biosorbed at time t and A and B are the intercept and Elovich constants relating to the degree of surface covering and activation energy for chemisorption, respectively. This intercept and the constants were determined using the linear plot of qt vs lnt. The plot of qt vs. ln t in Figure 7 provides the values of A and B. A summary of the values of A, B, and respective R^2 can be found in Table 2. High R^2 values in the experimental data indicate that the Elovich equation can be used to predict the adsorption

of CR dye on KPH cellulose. The validity of the Elovich equation further implies that the CR's adsorption was chemisorption [47].

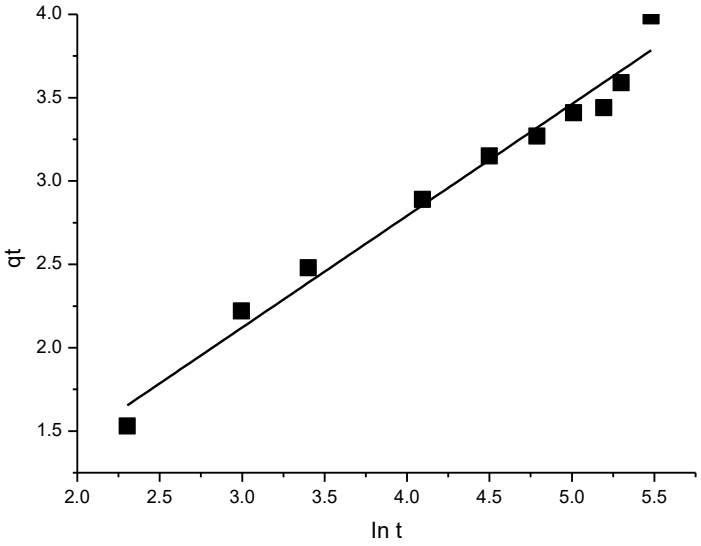

Figure 7: Elovich plots of CR dye adsorption on KPH cellulose

Table 2: Kinetic parameters for the biosorption of CR onto KPH cellulose

	Present study		Other studies	
Kinetic Model	Parameter	CR	[48]	[49]
Pseudo-first order	q_e(mgg^{-1})	9.65	0.52	---------
	K_1(min^{-1})	1.47 x 10^{-2}	0.007	---------
	R^2	0.486	0.3087	--------
Pseudo-second order	q_e (mg g^{-1})	2.78	8.65	4.44
	K_2(g mg^{-1} min^{-1})	2.73 x 10^{-2}	0.169	0.00154 x 10^{-3}
	R^2	0.9978	0.9997	0.9950
Elovich	A	10.37	--------	3.22
	B	2.98	--------	0.083
	R^2	0.9997	---------	0.9960

CONCLUSION

The adsorption of CR dye by KPH cellulose was studied due to the recent interest in developing cheap biomaterials for the removal of organic dyes from wastewaters. To do this, the CR dye's adsorption process, isotherms, and kinetics on KPH cellulose were investigated. Adsorbent dose, contact time pH, and dye concentration all played significant roles in controlling the adsorption process. As contact time, dose, and pH were increased, the percentage of CR dye removal also rose to optimum values and thereafter decreased. The fitting of experimental data to the Freundlich and Langmuir adsorption isotherm models suggests that monolayer and multilayer adsorption processes took place at room temperature. The pseudo-second order and Elovich model best describe the kinetics data indicating that chemisorption is the rate limiting step. Overall, it could be concluded that the prepared KPH cellulose adsorbent will be a promising adsorbent for the elimination of CR dye from aqueous solutions

Acknowledgment

The authors appreciate the technologists from Department of Chemical Sciences, Tai Solarin University of Education, Ijagun, Ogun State, Nigeria during the course of this study.

REFERENCES

1. Swan, N. B. & Zaini, M. A. A. (2019). Adsorption of malachite green and congo red dyes from water: recent progress and future outlook. *Ecological chemistry and engineering S*, *26*(1), 119-132.
2. Thinakaran, N., Panneerselvam, P., Baskaralingam, P., Elango, D. & Sivanesan, S. (2008). Equilibrium and kinetic studies on the removal of Acid Red 114 from aqueous solutions using activated carbons prepared from seed shells. *Journal of Hazardous Materials*, *158*(1), 142-150.
3. Shukla, R., Dubey, A., Pandey, V., Golhani, D. & Jain, A. P. (2012). Chromophore-an utility in uv spectrophotometer. *Inventi Rapid: Pharm Ana & Qual Assur*, *2012*(3), 1-4.
4. Gürses, A., Açıkyıldız, M., Güneş, K., Gürses, M. S., Gürses, A., Açıkyıldız, M., ... & Gürses, M. S. (2016). Dyes and pigments: their structure and properties. *Dyes and pigments*, 13-29.
5. Saini, R. D. (2018). Synthetic textile dyes: constitution, dying process and environmental impacts. *Asian Journal of Research in Chemistry*, *11*(1), 206-214.

6. Saratale, R. G., Saratale, G. D., Chang, J. S. & Govindwar, S. P. (2011). Bacterial decolorization and degradation of azo dyes: a review. *Journal of the Taiwan Institute of Chemical Engineers*, *42*(1), 138-157.
7. Ciardelli, F., Ruggeri, G., & Pucci, A. (2013). Dye-containing polymers: methods for preparation of mechanochromic materials. *Chemical Society Reviews*, *42*(3), 857-870.
8. Pavithra, K. G. & Jaikumar, V. J. J. O. I. (2019). Removal of colorants from wastewater: A review on sources and treatment strategies. *Journal of Industrial and Engineering Chemistry*, *75*, 1-19.
9. Kishor, R., Purchase, D., Saratale, G. D., Saratale, R. G., Ferreira, L. F. R., Bilal, M. & Bharagava, R. N. (2021). Ecotoxicological and health concerns of persistent coloring pollutants of textile industry wastewater and treatment approaches for environmental safety. *Journal of Environmental Chemical Engineering*, *9*(2), 105012.
10. Gautam, D., Kumari, S., Ram, B., Chauhan, G. S. & Chauhan, K. (2018). A new hemicellulose-based adsorbent for malachite green. *Journal of environmental chemical engineering*, *6*(4), 3889-3897.
11. Qadir, I. & Chhipa, R. C. (2015). Critical evaluation of some available treatment techniques for textile & paper industry effluents: a review. *American Chemical Science Journal*, *6*(2), 77-90.
12. Jiang, F., Dinh, D. M. & Hsieh, Y. L. (2017). Adsorption and desorption of cationic malachite green dye on cellulose nanofibril aerogels. *Carbohydrate polymers*, *173*, 286-294.
13. Shirsath, D. S. & Shrivastava, V. S. (2012). Removal of hazardous dye Ponceau-S by using chitin: An organic bioadsorbent. *African Journal of Environmental Science and Technology*, *6*(2), 115-124.
14. Malik, D. S., Sharma, A. K., Sharma, A. K., Thakur, R., & Sharma, M. (2020). A review on impact of water pollution on freshwater fish species and their aquatic environment. *Advances in environmental pollution management: wastewater impacts and treatment technologies*, *1*, 10-28.
15. Hernández-Zamora, M., Perales-Vela, H. V., Flores-Ortíz, C. M. & Cañizares-Villanueva, R. O. (2014). Physiological and biochemical responses of *Chlorella vulgaris* to Congo Red. *Ecotoxicology and Environmental Safety*, *108*, 72-77.
16. Xu, R., Mao, J., Peng, N., Luo, X., & Chang, C. (2018). Chitin/clay microspheres with hierarchical architecture for highly efficient removal of organic dyes. *Carbohydrate polymers*, *188*, 143-150.

17. Wanyonyi, W. C., Onyari, J. M., Shiundu, P. M. & Mulaa, F. J. (2019). Effective biotransformation of reactive black 5 dye using crude protease from *Bacillus cereus* strain KM201428. *Energy Procedia*, *157*, 815-824.
18. Nadeem, K., Guyer, G. T., Keskinler, B. & Dizge, N. (2019). Investigation of segregated wastewater streams reusability with membrane process for textile industry. *Journal of Cleaner Production*, *228*, 1437-1445.
19. Jia, Y., Ding, L., Ren, P., Zhong, M., Ma, J. & Fan, X. (2020). Performances and mechanism of methyl orange and Congo red adsorbed on the magnetic ion-exchange resin. *Journal of Chemical & Engineering Data*, *65*(2), 725-736.
20. Zhu, H. & Chen, Z. (2021). Preparation of MWCNT-MnO_2/Ni foam composite electrode for electrochemical degradation of Congo red wastewater. *International Journal of Electrochemical Science*, *16*(5), 210526.
21. Ramírez, G., Recio, F. J., Herrasti, P., Ponce-de-León, C. & Sires, I. (2016). Effect of RVC porosity on the performance of PbO_2 composite coatings with titanate nanotubes for the electrochemical oxidation of azo dyes. *Electrochimica Acta*, *204*, 9-17.
22. Wong, S., Tumari, H. H., Ngadi, N., Mohamed, N. B., Hassan, O., Mat, R. & Amin, N. A. S. (2019). Adsorption of anionic dyes on spent tea leaves modified with polyethyleneimine (PEI-STL). *Journal of cleaner production*, *206*, 394-406.
23. Aljeboree, A. M. & Alshirifi, A. N. (2018). Adsorption of Pharmaceuticals as emerging contaminants from aqueous solutions on to friendly surfaces such as activated carbon: A review. *Journal of Pharmaceutical Sciences and Research*, *10*(9), 2252-2257.
24. Chikri, R., Elhadiri, N., Benchanaa, M. & Maguana, Y. (2020). Efficiency of sawdust as low-cost adsorbent for dyes removal. *Journal of Chemistry*, *2020*, 1-17.
25. Salahuddin, N., Abdelwahab, M. A., Akelah, A. & Elnagar, M. (2021). Adsorption of Congo red and crystal violet dyes onto cellulose extracted from Egyptian water hyacinth. *Natural Hazards*, *105*, 1375-1394.
26. Mulushewa, Z., Dinbore, W. T. & Ayele, Y. (2021). Removal of methylene blue from textile waste water using kaolin and zeolite-x synthesized from Ethiopian kaolin. *Environmental Analysis, Health and Toxicology*, *36*(1): e2021007-0
27. Phele, M. J., Ejidike, I. P. & Mtunzi, F. M. (2019). Adsorption efficiency of activated macadamia nutshell for the removal of Organochlorine pesticides: Endrin and 4, 4-DDT from aqueous solution. *Journal of Pharmaceutical Sciences and Research*, *11*(1), 258-262.

28. Felista, M. M., Wanyonyi, W. C. & Ongera, G. (2020). Adsorption of anionic dye (Reactive Black 5) using macadamia seed husks: kinetics and equilibrium studies. *Scientific African*, *7*, e00283.
29. Errais, E., Duplay, J., Darragi, F., M'Rabet, I., Aubert, A., Huber, F. & Morvan, G. (2011). Efficient anionic dye adsorption on natural untreated clay: Kinetic study and thermodynamic parameters. *Desalination*, *275*(1-3), 74-81.
30. Nejib, A., Joelle, D., Fadhila, A., Sophie, G. & Malika, T. A. (2015). Adsorption of anionic dye on natural and organophilic clays: effect of textile dyeing additives. *Desalination and water treatment*, *54*(6), 1754-1769.
31. Wanyonyi, W. C., Onyari, J. M. & Shiundu, P. M. (2014). Adsorption of Congo red dye from aqueous solutions using roots of Eichhornia crassipes: kinetic and equilibrium studies. *Energy Procedia*, *50*, 862-869.
32. Ogunneye, A. L., Ibikunle, A. A., Sanyaolu, N. O., Yussuf, S. T., Gbadamosi, M. R., Badejo, O. A. & Lawal, O. S. (2020). Optimized carboxymethyl cellulose preparation from cocoa pod husks by surface response methodology. *Journal of Chemical Society of Nigeria*, *45*(1).
33. Wekoye, J. N., Wanyonyi, W. C., Wangila, P. T. & Tonui, M. K. (2020). Kinetic and equilibrium studies of Congo red dye adsorption on cabbage waste powder. *Environmental Chemistry and Ecotoxicology*, *2*, 24-31.
34. Bartošová, A., Blinová, L., Sirotiak, M., & Michalíková, A. (2017). Usage of FTIR-ATR as non-destructive analysis of selected toxic dyes. *Research Papers Faculty of Materials Science and Technology Slovak University of Technology*, *25*(40), 103-111.
35. Chakraborty, S., Mukherjee, A., Das, S., Maddela, N. R., Iram, S. & Das, P. (2021). Study on isotherm, kinetics, and thermodynamics of adsorption of crystal violet dye by calcium oxide modified fly ash. *Environmental Engineering Research*, *26*(1).
36. Chaari, I., Fakhfakh, E., Medhioub, M. & Jamoussi, F. (2019). Comparative study on adsorption of cationic and anionic dyes by smectite rich natural clays. *Journal of Molecular Structure*, *1179*, 672-677.
37. Kamran, U., Bhatti, H. N., Noreen, S., Tahir, M. A. & Park, S. J. (2022). Chemically modified sugarcane bagasse-based biocomposites for efficient removal of acid red 1 dye: Kinetics, isotherms, thermodynamics, and desorption studies. *Chemosphere*, *291*, 132796.
38. Cao, J. S., Lin, J. X., Fang, F., Zhang, M. T. & Hu, Z. R. (2014). A new absorbent by modifying walnut shell for the removal of anionic dye: Kinetic and thermodynamic studies. *Bioresource technology*, *163*, 199-205.

39. Ghaedi, M., Nasab, A. G., Khodadoust, S., Rajabi, M. & Azizian, S. (2014). Application of activated carbon as adsorbents for efficient removal of methylene blue: Kinetics and equilibrium study. *Journal of Industrial and Engineering Chemistry*, *20*(4), 2317-2324.
40. Ghaedi, M., Ghaedi, A. M., Negintaji, E., Ansari, A., Vafaei, A. & Rajabi, M. (2014). Random forest model for removal of bromophenol blue using activated carbon obtained from Astragalus bisulcatus tree. *Journal of Industrial and Engineering Chemistry*, *20*(4), 1793-1803.
41. Cheruiyot, G. K., Wanyonyi, W. C., Kiplimo, J. J. & Maina, E. N. (2019). Adsorption of toxic crystal violet dye using coffee husks: Equilibrium, kinetics and thermodynamics study. *Scientific African*, *5*, e00116.
42. Langmuir, I. (1918). The adsorption of gases on plane surfaces of glass, mica and platinum. *Journal of the American Chemical Society*, *40*(9), 1361-1403.
43. Adigun, O. A., Oninla, V. O., Babarinde, N. A., Oyedotun, K. O. & Manyala, N. (2020). Characterization of sugarcane leaf-biomass and investigation of its efficiency in removing Nickel (II), Chromium (III) and Cobalt (II) ions from polluted water. *Surfaces and Interfaces*, *20*, 100621.
44. Ibikunle, A. A., Ogunneye, A. L., Sanyaolu, N. O., Olutayo, K. A., Ogundare, S. A., Ogunmoye, A. O. & Moberuagba, K. H. (2023). Application of modified cellulose for Pb^{2+} and Cu^{2+} removal from aqueous solutions: Kinetic and isotherms studies. *Scientia Africana*, *22*(1), 115-132.
45. Ahmad, R. & Mirza, A. (2018). Synthesis of Guar gum/bentonite a novel bionanocomposite: Isotherms, kinetics and thermodynamic studies for the removal of Pb (II) and crystal violet dye. *Journal of molecular liquids*, *249*, 805-814.
46. Unya, I. U. (2021). The Historical Significance and Role of the Kola Nut among the Igbo of Southeastern Nigeria. *Journal of religion and human relations*, *13*(1), 289-312.
47. Klusacek, K., Hudgins, R. R. & Silveston, P. L. (1989). Multiple steady states of an isothermal catalytic reaction with Elovich adsorption. *Chemical Engineering Science*, *44*(10), 2377-2381.
48. Chang, M. Y. & Juang, R. S. (2005). Equilibrium and kinetic studies on the adsorption of surfactant, organic acids and dyes from water onto natural biopolymers. *Colloids and Surfaces A: Physicochemical and Engineering Aspects*, *269*(1-3), 35-46.
49. Arnata, I. W., Suprihatin, S., Fahma, F., Richana, N. & Sunarti, T. C. (2019). Adsorption of anionic congo red dye by using cellulose from sago frond. *Poll Res*, *38*(3), 43-53.
50. Samiey, B. & Dargahi, M. R. (2010). Kinetics and thermodynamics of adsorption of Congo red on cellulose. *Central European Journal of Chemistry*, *8*, 906-912.